



HAL
open science

Compact Planar Beamformer Using Multiple Continuous Parallel-Plate Waveguide Delay Lenses

François Doucet, Nelson J. G. Fonseca, Etienne Girard, Xavier Morvan,
Ronan Sauleau

► **To cite this version:**

François Doucet, Nelson J. G. Fonseca, Etienne Girard, Xavier Morvan, Ronan Sauleau. Compact Planar Beamformer Using Multiple Continuous Parallel-Plate Waveguide Delay Lenses. *IEEE Antennas and Wireless Propagation Letters*, 2022, 21 (11), pp.2229-2233. 10.1109/LAWP.2022.3184395 . hal-03884454

HAL Id: hal-03884454

<https://hal.science/hal-03884454v1>

Submitted on 1 Mar 2023

HAL is a multi-disciplinary open access archive for the deposit and dissemination of scientific research documents, whether they are published or not. The documents may come from teaching and research institutions in France or abroad, or from public or private research centers.

L'archive ouverte pluridisciplinaire **HAL**, est destinée au dépôt et à la diffusion de documents scientifiques de niveau recherche, publiés ou non, émanant des établissements d'enseignement et de recherche français ou étrangers, des laboratoires publics ou privés.



Distributed under a Creative Commons Attribution - NonCommercial 4.0 International License

Compact Planar Beamformer Using Multiple Continuous Parallel Plate Waveguide Delay Lenses

François Doucet, Nelson J. G. Fonseca, *Senior Member, IEEE*, Etienne Girard, Xavier Morvan and Ronan Sauleau, *Fellow, IEEE*

Abstract—A compact planar beamformer using multiple shaped continuous parallel plate waveguide delay lenses is proposed in this letter. The original design, based on a single shaped continuous delay lens, had demonstrated excellent scanning properties over the portion of the K_a -band allocated to uplink satcom (27.5–31 GHz). However, its height, due to the transversal ridge and cavity, was limiting its use in more advanced antenna systems. A design methodology is proposed here to achieve similar focusing properties while reducing significantly the beamformer’s height. A specific design is demonstrated with a height reduced by a factor of 3 when compared to the original design. A reduction of the longitudinal dimension is also proposed by introducing two additional straight ridges and cavities. A prototype was manufactured and tested successfully, with RF performance similar to those of the reference design besides slightly higher insertion losses. This compact design enables to stack multiple lenses to produce two-dimensional beamforming.

Index Terms—Geometrical optics (GO), line source, multiple beam antenna, parallel plate waveguide (PPW) beamformer.

I. INTRODUCTION

LOW and medium Earth orbit satellite constellations under development require beamforming solutions with a large field of view (typically from $\pm 30^\circ$ to $\pm 60^\circ$) and wide or multiple frequency band capability. Quasi-optical beamformers, first introduced in the 1950s for radar applications, provide such characteristics while representing a low cost alternative to phased array antennas [1]. The pillbox antenna [2], still investigated for high frequency applications up to sub-terahertz [3]–[5], is attractive for its very simple parallel plate waveguide (PPW) design. The Rotman lens [6] was introduced to enhance the scanning capabilities of PPW beamformers, with low aberrations up to about $\pm 30^\circ$ in azimuth, possibly extendable with an adequate design of the focal curve [7]. The Luneberg lens [8] provides even wider scanning range

This work was supported in part by the European Space Agency (ESA) and in part by Thales Alenia Space, France, in the frame of ESA’s Networking/Partnering Initiative (NPI).

F. Doucet was with Univ Rennes, CNRS, IETR (Institut d’Electronique et de Technologies du Numérique) – UMR 6164, F-35000 Rennes, France and is now with Dassault Aviation, Saint Cloud, France (e-mail: Francois.Doucet@dassault-aviation.com).

N. J. G. Fonseca is with the European Space Agency, 220 AG Noordwijk, The Netherlands (e-mail: nelson.fonseca@esa.int).

X. Morvan and R. Sauleau are with Univ Rennes, CNRS, IETR (Institut d’Electronique et de Technologies du Numérique) – UMR 6164, F-35000 Rennes, France (e-mail: ronan.sauleau@univ-rennes1.fr).

E. Girard is with the Research and Development Department, Thales Alenia Space, 31037 Toulouse, France (e-mail: etienne.girard@thalesalenaspace.com).

in theory with its rotationally symmetric focusing properties, but the various techniques described to synthesize its graded index [9], [10] become quite challenging and lossy at high frequencies. Solutions based on the geodesic lens, also known as the Rinehart–Luneburg lens [11], [12], were proposed in [13]–[16] for space and terrestrial applications.

The novel PPW beamformer introduced in [17] proves to be a good compromise between the pillbox antenna and the Rotman lens. This beamformer transforms a cylindrical wave launched in a PPW section into a quasi-plane wave and vice-versa, by using a PPW lens formed of a continuous transversal ridge and cavity. The concept avoids the discretization required by the Rotman lens which introduces inherently bandwidth and scanning limitations due to grating lobes. A specific analytical model based on geometrical optics (GO), improving the original bifocal constrained lens approximation [18], was described in [19], providing fast and accurate prediction of the radiating properties and enabling the use of optimization procedures [20]. The elliptical inner lens and ridge profiles derived from the bifocal constrained lens approximation were replaced by shaped polynomial profiles to improve further the scanning performance and pattern shape [21], achieving low phase aberration levels over an angular range similar to those obtained with a classical Rotman lens with a much simpler mechanical design. The main drawback of this solution is its height (typically 2λ , where λ is the wavelength in free space), due to the transversal ridge and cavity. A value below λ is desirable to enable beamforming along the orthogonal direction with a stack of lenses.

In this letter, we explore the possibility to distribute the transversal height over several and separate ridges and cavities to reduce the beamformer’s height. The key contribution of this work is to demonstrate that the single delay lens implemented in [21] can be replaced by multiple transversal lenses. A significant height reduction is achieved while preserving the focusing properties and the wide frequency bandwidth.

II. COMPACT CONTINUOUS LENS DESIGN

The design proposed is presented in Fig. 1. The main parameters are identical to those defined in [21] for the single-lens prototype. The lens diameter and the off-axis focal distance are set to $D = 10\lambda$ and $f = 0.7D$, respectively, where λ is the wavelength in free space at the minimum operating frequency $f = 27.5$ GHz. The angles θ_1 and θ_2 define the angular feed position and the corresponding beam pointing direction, respectively. The GO tool developed in our

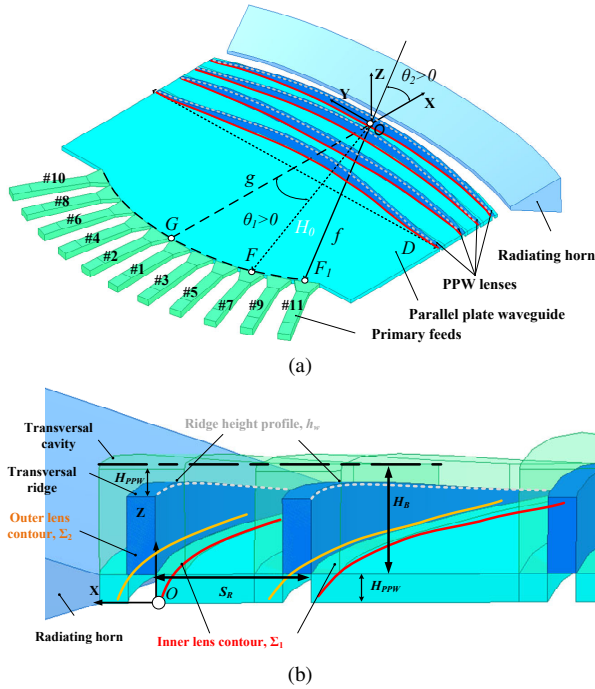


Fig. 1. Continuous PPW lens-like beamformer based on multiple delay lenses: (a) 3D view, (b) zoom on the ridges and cavities.

previous works [19], [21] was upgraded to enable multiple ridges. It was found that the GO approximation and model simplifications (e.g. locally planar ridge with straight line propagation) remain valid, provided successive ridges are not too close to each other. This enables to speed up significantly the design process also in this case when compared to a full-wave optimisation approach [20]. With the considered design parameters, up to four ridges and cavities may be cascaded maintaining accurate prediction of radiating patterns and reasonable convergence times. To provide an adequate cross-over level between adjacent beams (typically less than 3 dB) while maintaining low side lobe level (SLL), an approach similar to the one implemented in [21] and inspired from the works on Rotman lenses [22], [23] is considered. The antenna system comprises two superimposed lenses with eleven beams for each lens ranging respectively from -28.5° to 31.5° and from -31.5° to 28.5° using a uniform angular step of 6° with feeds shifted half-a-step between the two lenses and designed in a symmetrical way so the two lenses are identical upon rotation of 180° around the main focal axis (x -axis in Fig. 1a).

As in previous designs, the radiating horn is conformed to the profile of the outer lens contour. A pattern-based optimization [20] is used to achieve the desired results at the central frequency $f_0 = 30$ GHz for the central feed ($\theta_1 = 1.5^\circ$) and the most scanned feed ($\theta_1 = 31.5^\circ$) simultaneously, while fixing the normalized on-axis focal distance g to 1 (Fig. 1a). For each beam, a half-power beamwidth (HPBW), θ_{3dB} , identical to the one obtained in the reference design [21] is targeted while minimizing SLL. In our previous designs, the parameter g was used to further lower aberrations across the focal arc, as commonly done in Rotman lens designs. However, this typically requires a value $g > 1$ [21]. Combined

with the constraint of pointing each feed towards the center of the aperture for an adequate illumination, this typically leads to asymmetric off-axis feed designs resulting in performance degradation. In this work, we take advantage of the added degrees of freedom thanks to the use of multiple lenses to achieve low phase aberrations over the scanning range while enforcing $g = 1$. Besides the fact that it simplifies the focal arc design, it also reduces slightly the overall length of the beamformer when compared to previously reported designs.

In the optimization process, each lens is translated along the x -axis by a distance S_R defined with reference to the coordinate system (O, x, y, z) set at the center of the aperture before the flare (Fig. 1a). A minimum distance equal to $\lambda = 10.9$ mm, the wavelength in free space at the lowest operating frequency, is assigned between the successive inner lens profiles (Σ_1) as a good compromise between compactness and accuracy of the ray-tracing model. This minimum distance also avoids strong standing waves between the different bend transitions and respects the accommodation constraints of the four transversal cavities considered. Due to the large number of variables, an iterative process is required as the result of the optimisation is sensitive to the initial guess condition. The goal is to progressively minimize each delay lens and thus the beamformer height H_B , while maintaining the desired far-field patterns. As shown in Fig. 1b, the parameter H_B is defined as the distance computed along z -axis between the upper plate of the parallel plate section and the maximum height of the transversal cavities. The final design is characterized by eight polynomial equations defining the inner lens contour (Σ_1) and the ridge height profile (h_w) of each lens. The final beamformer height obtained is $H_B = 7.5$ mm, compared to 20.5 mm for the reference design [21]. The FEM simulations performed using HFSS [24] to confirm the GO tool results demonstrate comparable RF characteristics (i.e. radiation patterns, S-parameters) as the ones obtained in [21]. The experimental validation is discussed in Section III.

III. COMPACT CONTINUOUS LENS PROTOTYPE

The final as-built design is presented in Fig. 2, using two blocks of aluminum and standard milling as in [21]. The reduced ridge height results in less material waste and facilitates the milling of the cavities. The four delay lenses used for enhanced compactness along the transversal direction are on the side of the aperture. In addition, two straight transversal ridges and cavities were added, folding up the longitudinal PPW section, to further reduced the length along the x -axis. The two transversal cavities are defined with the maximum beamformer height $H_B = 7.5$ mm, obtained with the GO optimization. Their relative position and distance with respect to the other parts of the structure (i.e. the delay lenses and the focal arc) have been optimized to avoid reflections at feed level and maintain the radiation patterns unchanged. The feeds provide a transition to standard waveguides WR28 for test purposes. The final as-built design considers metallic sidewalls in order to propose a simpler design and assembly process, and avoid the use of absorbing materials, as this was found to have limited impact on RF results [21]. The final dimension

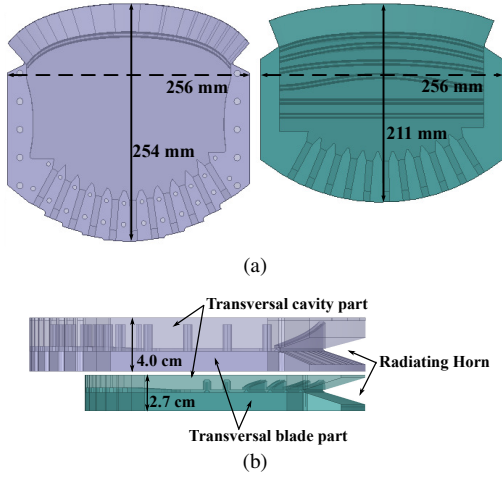


Fig. 2. CAD views of the compact continuous delay lens design (in dark green) compared to the reference single-lens design (in purple) [21]: (a) in-plane view and (b) transversal view.

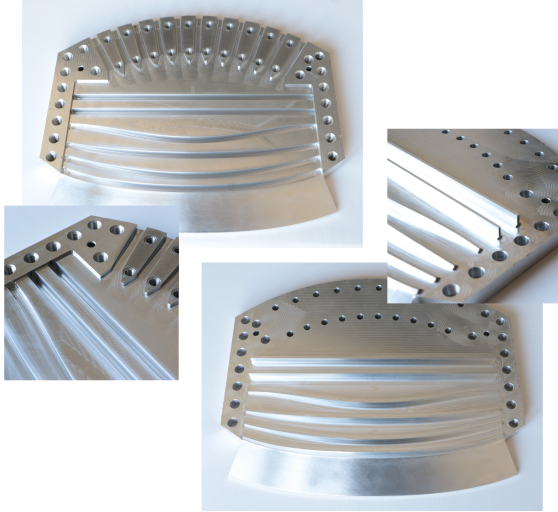


Fig. 3. Compact continuous delay lens prototype manufactured in two blocks: one with transversal cavities (top left) and one with ridges (bottom right), including respective close-up views.

along x -axis is 211 mm, instead of 254 mm with a single delay lens (Fig. 2a). The final transversal dimension (along z -axis) is 2.7 cm, instead of 4 cm (Fig. 2b). The reduction in the transversal direction is constrained by the horn aperture height (2 cm), chosen identical to the single-lens prototype for a fair comparison. The height of the PPW, $H_{PPW} = 2$ mm, is also the same as in the reference design, and is chosen to have the beamformer operating in its fundamental TEM mode only, resulting in a well-defined linear polarization along z -axis (see Fig. 1). As a consequence, the simulated and measured cross-polarized signals are very low (typically 40 dB below the peak directivity) and are not reported in this letter.

The two blocks before assembly are visible in Fig. 3, including close-up views on the ridges and cavities. The antenna was measured in the compact antenna test range (CATR) at ESA/ESTEC, The Netherlands. The H-plane radiation patterns measured at $f_0 = 30$ GHz for the central and the extreme feeds

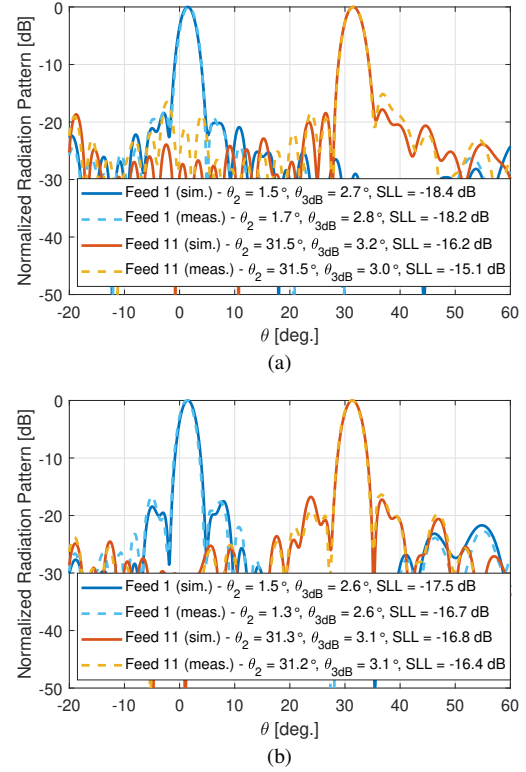


Fig. 4. H-plane normalized radiation patterns of the PPW beamformer at $f_0 = 30$ GHz for the feed 1 ($\theta_1 = 1.5^\circ$) and the feed 11 ($\theta_1 = 31.5^\circ$) for (a) the compact lens and (b) the reference single-lens design [21].

(ports 1 and 11) are reported in Fig. 4a. They are compared to the FEM simulation results. As a reference, the same results are provided for the single-lens design [21] in Fig. 4b. For feed 1, a good agreement is observed in the main lobe and the first side lobes. The main beam pointing direction is 1.5° and 1.7° for the FEM simulation and the measured results, respectively. The corresponding HPBW values are 2.7° and 2.8° , while the SLL is -18.4 dB and -18.2 dB, respectively. The main beam is slightly wider with lower SLL with reference to the single-lens design (Fig. 4b). For feed 11, the comparison demonstrates also a good agreement in the main lobe with main beam directions equaling 31.5° and an HPBW of 3.2° , 3.0° for the FEM and the measured results, respectively. Concerning SLL, a slight imbalance is observed in measurements and a degradation from -16.2 dB to -15.1 dB when compared to simulation results. The compact design with multiple lenses is expected to be more sensitive to manufacturing errors as small discrepancies accumulate along the beamformer, compared to the single-lens design with a mostly flat beamforming design. This may explain the small differences observed. The results are still considered very good for a first demonstration.

The measured directivity and realized gain values are compared to directivities computed with the FEM simulation assuming PEC material for both the central feed 1 ($\theta_1 = 1.5^\circ$) and the extreme feed 11 ($\theta_1 = 31.5^\circ$) in Fig. 5. The measured and simulated directivities are in good agreement. The realized gain is around 0.6 dB below directivity for the compact design (about 0.2 dB for a single-lens design [21]). These additional

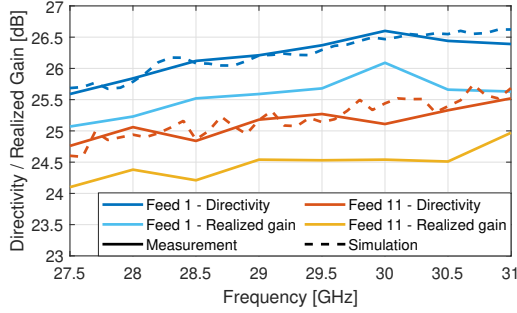


Fig. 5. Directivity and realized gain versus frequency of the compact continuous lens for the feed 1 ($\theta_1 = 1.5^\circ$) and the feed 11 ($\theta_1 = 31.5^\circ$).

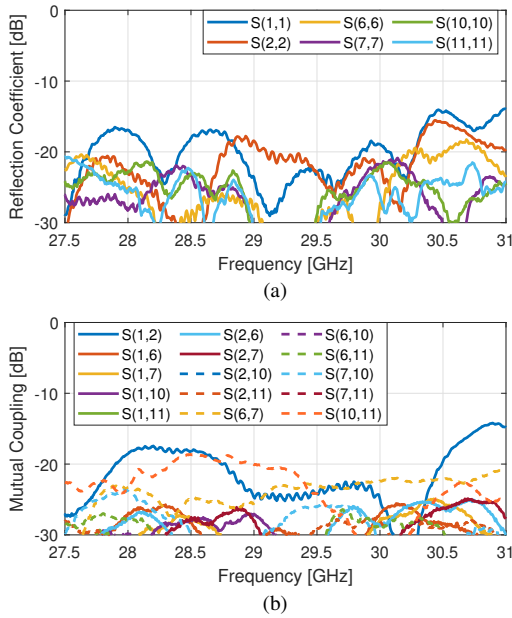


Fig. 6. Measured S-parameters of the compact continuous lens over the entire K_a up-link frequency band, (a) reflection and (b) mutual coupling coefficients.

losses are due to the multiple ridges resulting principally in an increase of the coupling between the different feeds and multiple reflections in the PPW cavity. These results are very good considering the number of ridges (6 instead of 1) and the size reduction achieved, preserving the low-loss figure of this fully metallic solution. Measured scattering parameters are reported in Fig. 6, including reflection and mutual coupling coefficients for selected feeds. The reflection coefficients are similar to those obtained with the single-lens prototype [21], typically below -20 dB except for the central feeds 1 and 2 where the levels are slightly higher, affected by the first straight ridge. Mutual coupling is also mostly below -20 dB except between feeds located almost symmetrically with respect to x -axis (e.g. 1, 2 and 10, 11). This is a consequence of specular reflection on the first straight ridge. The degradation of performance remains fairly acceptable in view of the significant volume reduction. Finally, contour plots for an antenna system comprising two symmetric lenses as discussed in [21] are reported in Fig. 7, showing good overlap between adjacent beams along the azimuth angle. The

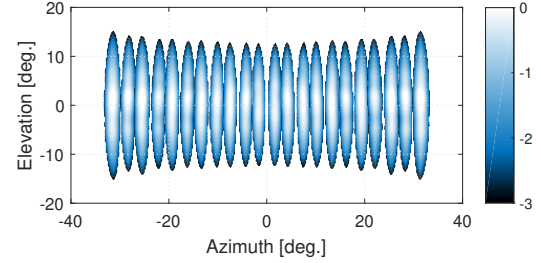


Fig. 7. Measured 3 dB contour plots of the compact continuous lens at $f_0 = 30$ GHz for all the feeds and for the same beamformer with a 180° rotation around x -axis [21].

main characteristics of the proposed beamformer are listed in Table I, and compared to alternative quasi-optical designs.

TABLE I
COMPARISON OF QUASI-OPTICAL PPW BEAMFORMERS

Ref.	Beamformer type	F/D^a	Height ^b	Scanning range	Scan loss
[2]	Pillbox	0.5	N/A	$\pm 50^\circ$	2.5 dB
[7]	Rotman lens	0.7	N/A	$\pm 50^\circ$	2 dB
[14]	Rinehart-Luneburg lens	1	1.1λ	$\pm 75^\circ$	2 dB
[15]	Half-Luneburg lens	0.5	1.1λ	$\pm 30^\circ$	1-2 dB
[21]	Single delay lens	0.7	1.9λ	$\pm 35^\circ$	1-1.5 dB
This work	Multiple delay lens	0.6	0.7λ	$\pm 35^\circ$	1-1.5 dB

^aexcluding the flare horn and feeds; ^bexcluding the height of the flare horn. λ is the wavelength at the lowest reported operating frequency.

IV. CONCLUSION

This letter described a shaped continuous PPW delay lens beamformer with reduced dimensions thanks to multiple ridges and cavities. A compact design with a height of only 7.5 mm was validated, corresponding to a reduction by a factor 2.7 compared to the reference concept. This volume reduction preserves RF results. These were validated experimentally at K_a -band, with very similar results when compared to the single-lens prototype. The design maintains a high efficiency, with insertion losses of about 0.6 dB, due to the more complex structure. Using two stacked lenses to provide adequate cross over levels, the final transversal dimension is reduced to 54 mm (80 mm with the reference lens design) and is in this case limited by the aperture horn dimension. Further size reduction by increasing the number of ridges would be needed to enable elevation scanning using a stack of paired lenses without appearance of undesired grating lobes. This would require to update the modelling approach to maintain accurate and fast predictions in order to perform adequate optimizations.

ACKNOWLEDGMENTS

The authors would like to thank Dr. Hervé Legay, from Thales Alenia Space, for valuable feedback on this work as well as Eric van der Houwen and Ines Barbary, both from ESA, for handling the test campaign in the CATR.

REFERENCES

- [1] Y. J. Guo, M. Ansari, R. W. Ziolkowski and N. J. G. Fonseca, "Quasi-Optical Multi-Beam Antenna Technologies for 5G and 6G mmWave and THz Networks: A Review," *IEEE Open J. Antennas Propag.*, vol. 2, pp. 807-830, June 2021.
- [2] W. Rotman, "Wide-angle scanning with microwave double-layer pill-boxes," *IRE Trans. Antennas Propag.*, vol. 6, no. 1, pp. 96-105, Jan. 1958.
- [3] T. Potelon, M. Ettorre, T. Bateman, J. Francey, and R. Sauleau, "Broad-band passive two-feed-per-beam pillbox architecture for high beam cross-over level," *IEEE Trans. Antennas Propag.*, vol. 68, no. 1, pp. 575-580, Jan. 2020.
- [4] A. Gomez-Torrent *et al.*, "A Low-Profile and High-Gain Frequency Beam Steering Subterahertz Antenna Enabled by Silicon Micromachining," *IEEE Trans. Antennas Propag.*, vol. 68, no. 2, pp. 672-682, Feb. 2020.
- [5] G. Sun and H. Wong, "A Planar Millimeter-Wave Antenna Array With a Pillbox-Distributed Network," *IEEE Trans. Antennas Propag.*, vol. 68, no. 5, pp. 3664-3672, May 2020.
- [6] W. Rotman and R. Turner, "Wide-angle microwave lens for line source applications," *IEEE Trans. Antennas Propag.*, vol. 11, no. 6, pp. 623-632, Nov. 1963.
- [7] N. J. G. Fonseca, "A Focal Curve Design Method for Rotman Lenses With Wider Angular Scanning Range," *IEEE Antennas Wirel. Propag. Lett.*, vol. 16, pp. 54-57, 2017.
- [8] R. K. Luneburg, *Mathematical Theory of Optics*. Providence, RI, USA: Brown Univ., 1944.
- [9] C. D. Diallo, E. Girard, H. Legay, and R. Sauleau, "All-metal Ku-band Luneburg lens antenna based on variable parallel plate spacing fakir bed of nails," in *Proc. 11th Eur. Conf. Antennas Propag. (EUCAP)*, Paris, France, Mar. 2017, pp. 1401-1404.
- [10] O. Quevedo-Teruel, J. Miao, M. Mattsson, A. Algaba-Brazalez, M. Johansson, and L. Manholm, "Glide-symmetric fully metallic Luneburg lens for 5G communications at Ka-Band," *IEEE Antennas and Wireless Propag. Lett.*, vol. 17, no. 9, pp. 1588-1592, Sept. 2018.
- [11] R. F. Rinehart, "A solution of the problem of rapid scanning for radar antennas," *J. Appl. Phys.*, vol. 19, pp. 860-862, Oct. 1948.
- [12] R. F. Rinehart, "A family of designs for rapid scanning radar antennas," *Proc. IRE*, vol. 40, no. 6, pp. 686-688, June 1952.
- [13] Q. Liao, N. J. G. Fonseca, and O. Quevedo-Teruel, "Compact multibeam fully metallic geodesic Luneberg lens based on non-euclidian transformation optics," *IEEE Trans. Antennas Propag.*, vol. 66, no. 12, pp. 7383-7388, Dec. 2018.
- [14] N. J. G. Fonseca, Q. Liao and O. Quevedo-Teruel, "Equivalent Planar Lens Ray-Tracing Model to Design Modulated Geodesic Lenses Using Non-Euclidean Transformation Optics," *IEEE Trans. Antennas Propag.*, vol. 68, no. 5, pp. 3410-3422, May. 2020.
- [15] N. J. G. Fonseca, Q. Liao and O. Quevedo-Teruel, "Compact parallel-plate waveguide half-Luneburg geodesic lens in the Ka-band," *IET Microw. Antennas Propag.*, vol. 15, no. 2, pp. 123-130, Feb. 2021.
- [16] N. J. G. Fonseca, "The water drop lens: revisiting the past to shape the future," *EurAAP Reviews Electromag.*, vol. 1, no. 1, pp. 1-4, Jan. 2022.
- [17] H. Legay *et al.*, "Multiple beam antenna based on a parallel plate waveguide continuous delay lens beamformer," in *Proc. Int. Symp. Antennas Propag.*, Okinawa, Japan, Oct. 2016, pp. 118-119.
- [18] N. J. G. Fonseca *et al.*, "Continuous parallel plate waveguide beamformer based on a bifocal constrained lens design," *IEEE Int. Symp. Antennas Propag. (APSURSI)*, Jun. 2016, pp. 1347-1348.
- [19] F. Doucet, N.J.G. Fonseca, E. Girard, H. Legay, and R. Sauleau, "Analytical model and study of continuous parallel plate waveguide lens-like multiple beam antennas," *IEEE Trans. Antennas Propag.*, vol. 66, no. 9, pp. 4426-4436, Aug. 2018.
- [20] F. Doucet, N.J.G. Fonseca, E. Girard, H. Legay, and R. Sauleau, "Comparison of optimization procedures for the design of continuous parallel plate waveguide multiple beam lens antennas," in *Proc. 10th Eur. Conf. Antennas Propag. (EUCAP)*, London, United Kindom, Apr. 2018, pp. 1-5.
- [21] F. Doucet *et al.*, "Shaped continuous parallel plate delay lens with enhanced scanning performance," *IEEE Trans. Antennas Propag.*, vol. 67, no. 11, pp. 6695-6704, Nov. 2019.
- [22] K. Kee Chan and S. Rao, "Design of a Rotman lens feed network to generate a hexagonal lattice of multiple beams," *IEEE Trans. Antennas Propag.*, vol. 50, no. 8, pp. 1099-1108, Aug. 2002.
- [23] M. Maybell, K. Chan, and P. Simon, "Rotman lens recent developments 1994-2005," in *Proc. IEEE Antennas Propag. Soc. Int. Symp.*, pp. 27-30. Dec. 2005.
- [24] Ansoft HFSS version 18.0, 1984-2017, Ansoft Corporation.